Structural Analysis of a Novel Interaction by Calmodulin: High-Affinity Binding of a Peptide in the Absence of Calcium[†]

Jeffrey L. Urbauer,[‡] James H. Short,[‡] Linda K. Dow,[§] and A. Joshua Wand*[,‡,§]

Department of Biochemistry and Program in Biophysics, University of Illinois at Urbana−Champaign, Urbana, Illinois 61801

Received February 28, 1995; Revised Manuscript Received April 26, 1995[⊗]

ABSTRACT: The interaction of apocalmodulin (apoCaM) with a peptide (Neuro$_p$) based on the primary sequence of the calmodulin-binding domain of neuromodulin has been studied by nuclear magnetic resonance (NMR) methods. The NMR spectra of both apocalmodulin and its 1:1 complex with the Neuro$_p$ peptide have been assigned by triple resonance and nuclear Overhauser effect-(NOE-) based strategies. ApoCaM displays many of the same basic structural features as calcium-saturated calmodulin. Analysis of observed chemical shifts and patterns of NOEs on the main chain indicates extensive and regular secondary structure throughout the N-terminal domain. In contrast, the helices of the C-terminal domain are somewhat irregular and are dynamically averaged. The EF-hands are intact in the N-terminal domain with the loops forming a short antiparallel β sheet. Under low-salt conditions, two helix−loop−helix EF-hand motifs are present in the C-terminal domain of apoCaM but do not show interstrand NOEs. The spectral perturbations of apoCaM upon complexation with the Neuro$_p$ peptide are relatively small with the larger chemical shift perturbations occurring in the C-terminal domain. The general secondary structure and tertiary organization appears to remain roughly the same as in free apoCaM. Stoichiometric titration of the apoCaM•Neuro$_p$ complex with calcium indicates that the C-terminal domain EF-hands have a higher affinity for calcium than N-terminal domain EF-hands. Thus, this complex offers a unique opportunity to examine the structural and energetic consequences of calcium-dependent and calcium-independent binding of peptide to calmodulin.

Calmodulin (CaM)[1] is a small 16.7-kDa calcium-binding protein which is central to the regulation of a wide range of cellular responses. The crystal structure of calmodulin in the presence of excess calcium reveals an unusual dumbbell structure with two helix−loop−helix EF-hand metal-binding sites located in each of the two globular domains (Babu et al., 1988). A long, highly solvent exposed helix connects the two globular domains. Analysis of the solution conformation of calcium-saturated calmodulin indicates that this bridging or "central" helix is in fact locally dynamically disordered (Ikura et al., 1991b; Barbato et al., 1992) such that a "flexible tether" is created, as had been originally proposed (Persechini & Krestinger, 1988). This "flexible tether" is ultimately central to the recognition by calmodulin of at least two calmodulin-binding domains. The calcium-binding sites of calmodulin show a varying but relatively limited range of binding affinities (Minowa & Yagi, 1984). The binding of calcium is cooperative with respect to the two globular domains and has been proposed to promote a conformational change that exposes a hydrophobic surface to initiate binding of the target protein. Complexation of calcium-loaded calmodulin with peptides corresponding to the calmodulin-binding domains of regulated proteins has been studied in great detail. Peptides which comprise the CaM-binding domains of target proteins typically have the ability to form basic amphiphilic α-helices and bind CaM only in the presence of Ca^{2+} (O'Neil & De Grado, 1990). The amphiphilic helix model for the structure of a peptide corresponding to a calmodulin-binding domain bound to CaM was first directly confirmed by NMR-based studies on the complex of CaM with a peptide analog of the myosin light chain kinase CaM-binding domain (Roth et al., 1991). Subsequently, the structures of three CaM−peptide complexes were determined and found to adopt an unusual compact structure where the helical peptide is essentially buried between the two globular domains (Ikura et al., 1992; Meador et al., 1992, 1993). The interaction between the bound peptide and CaM in the compact complex involves both extensively buried salt linkages and general hydrophobic interactions. An emerging view of how the binding of peptides to CaM leads to the final structure is that the initial stages of molecular recognition are driven by relatively nonspecific hydrophobic interactions while the later stages require helix formation and creation of specific pairwise ionic interactions (Fisher et al., 1994; Ehrhardt et al., 1995). These pairwise interations drive the collapse of the initial encounter complex to the unusual compact structure where the helical peptide is essentially buried in between the two globular domains. Possible exceptions to this general mode of complexation are a pair of neural-specific proteins, neuro-

---

[†] This work was supported by NIH Research Grant DK-39806. L.K.D. is the recipient of an NIH predoctoral fellowship (GM-08276).

* Address all correspondence to this author at the Department of Biochemistry.

[‡] Department of Biochemistry.

[§] Program in Biophysics.

[⊗] Abstract published in *Advance ACS Abstracts,* June 1, 1995.

[1] Abbreviations: CaM, calmodulin; COSY, *J*-correlation spectroscopy; CSI, chemical shift index; DQF, double quantum filtered; FAB, fast atom bombardment; HSQC, heteronuclear single quantum coherence; MCD, main-chain directed; MLCK, myosin light-chain kinase; Neuro$_p$, peptide corresponding to the calmodulin-binding domain of neuromodulin as defined in the text; NMR, nuclear magnetic resonance; NOE, nuclear Overhauser effect; NOESY, NOE-correlation spectroscopy; pH*, pH uncorrected for the isotope effect; ppm, parts per million; tBOC, *tert*-butyloxycarbonyl; TMS, tetramethylsilane; TOCSY, total correlation spectroscopy.

0006-2960/95/0434-8099$09.00/0

modulin and neurogranin, which will bind CaM only in the absence of Ca^{2+} (Apel et al., 1990; Baudier et al., 1991). While the intact proteins do not bind with appreciable affinity to calcium-saturated CaM, the isolated peptides corresponding to the calmodulin-binding domains of the two proteins do bind to calcium-saturated CaM. Thus, although the model peptides do not entirely mimic the behavior of the intact protein from which they are derived, they do offer the opportunity to examine the origins of the calcium-dependent binding of peptide. The amino acid sequences of the CaM-binding regions of these proteins do not possess the pronounced potential for amphiphilic helix formation common to other CaM-binding domains, though they are dominated by hydrophobic and basic residues. Nevertheless, transferred NOE studies of the bound peptide indicate that a peptide corresponding to the calmodulin-binding domain of neuromodulin adopts a helical conformation while bound to apoCaM (Zhang et al., 1994). The structural consequences of the binding of this domain to apocalmodulin are unknown. Indeed, the structural details of apocalmodulin are also largely unknown. Circular dichroism studies indicate that apocalmodulin has a high secondary structure content similar to the calcium-saturated state (Martin & Bayley, 1986; Hennessey et al., 1987; Maune et al., 1992). A slight increase in helicity is indicated upon binding of calcium (Hennessey et al., 1987). Evidence has also been presented that is consistent with the presence of an interdomain interaction in apocalmodulin which is significantly reduced or absent in calcium-saturated CaM (Yao et al., 1994; Pedigo & Shea, 1995).

Here we present a study of the structural consequences of the binding of a peptide based on the sequence of the calmodulin-binding domain of neuromodulin to apocalmodulin. Main-chain NMR resonance assignments of both apocalmodulin and the 1:1 complex have been assigned by multidimensional NMR techniques. The resonance assignments of apoCaM reported here supplement the limited number of mostly side-chain resonance assignments obtained previously on intact and proteolytic fragments of apocalmodulin [e.g., Seamon (1980), Aulabaugh et al. (1984), Klevit et al. (1984), and Starovasnik et al. (1992)]. Analyses of the observed patterns of NOEs and chemical shifts allow for delineation of the regions of secondary structure of the apoCaM and the apoCaM·$Neuro_p$ complex and help explain previously reported observations. The influence of the presence of bound peptide on the binding of calcium to calmodulin is also examined and found to maintain the difference in binding affinity of the two globular domains. These and other results point to the structural origins of linked function in the basic calcium signal transduction mechanism.

MATERIALS AND METHODS

Preparation of Apocalmodulin. Escherichia coli EMG-2 cells harboring a plasmid containing the chicken calmodulin gene (Putkey et al., 1985) were grown on minimal medium (M9) containing uniformly ^{13}C-labeled glucose (99%, Cambridge Isotope Laboratories) as the sole carbon source and $^{15}NH_4Cl$ (99%, Isotec Inc.) as the sole nitrogen source, in a manner described previously (Roth et al., 1992). A sample labeled only with ^{15}N as well as two samples selectively enriched with α-^{15}N-labeled lysine or α-^{15}N -labeled leucine were also prepared using an amino acid cocktail as described previously (Roth et al., 1992). Calmodulin was isolated and purified by affinity chromatography on phenyl-Sepharose (Gopalakrishna & Anderson, 1982; Seeholzer & Wand, 1989). Apocalmodulin was prepared by dialysis against two 4-L volumes of buffer containing 0.05 mM EDTA. Residual calcium levels were determined to be less than 10 μM using antipyrylazo III (Budesinsky, 1974). Final NMR samples contained, in a volume of 0.55 mL, 5 mM KCl, 5 mM imidazole-d_4, 0.02% sodium azide, and 0.05 mM EDTA in 92% H_2O/8% D_2O at pH* 6.5. The protein concentrations for ^{15}N,^{13}C-apoCaM, ^{15}N -apoCaM, ^{15}N-labeled lysine apoCaM, and ^{15}N-labeled leucine apoCaM were 3, 4.5, 0.5, and 0.5 mM, respectively. A sample of unlabeled apoCaM (3 mM) was similarly prepared.

Preparation of the $Neuro_p$ Peptide. The peptide used in these studies was based on the sequence of the bovine neuromodulin calmodulin-binding domain (Chapman et al., 1991) with tryptophan substituted for wild-type phenylalanine at position four. The sequence of the peptide used is acetyl-QASWRGHITRKKLKGEK-NH_2; it was synthesized as an N-terminal acetylated and C-terminal amidated peptide by solid-phase techniques on an Applied Biosystems 430A peptide synthesizer using standard tBOC chemistry. The peptide ($Neuro_p$) was purified by reversed-phase HPLC and the purity and identity (molecular weight) were confirmed by FAB mass spectrometry.

Titration of ApoCaM with $Neuro_p$ Peptide. The ^{15}N,^{13}C-apoCaM·$Neuro_p$ sample used for resonance assignment work was prepared directly from a 3 mM stock solution of the peptide in pH-adjusted water and a 0.6 mM stock solution of apoCaM prepared in buffer. Complexation was directly confirmed by NMR spectroscopy. Complexes were generally prepared under dilute conditions and concentrated by lyophilization (Seeholzer & Wand, 1989). The complex was then lyophilized and brought to the required volume with 90% H_2O/10% D_2O to achieve the desired buffer concentration. It should be noted that under the conditions employed here both apoCaM and its complex with the $Neuro_p$ peptide are relatively unstable and showed significant spectral changes after approximately 2 months at room temperature.

Titration of ApoCaM with Salt. The effect of increasing ionic strength on the solution structure of apoCaM was investigated by titrating a solution of apoCaM with KCl. To a 0.55-mL sample of ^{15}N apoCaM (2.0 mM) in 5 mM imidazole-d_4, 0.05 mM EDTA, 0.02% NaN_3, 8% D_2O, and 5 mM KCl at pH 6.5 was added small aliquots of an identical solution (minus the apoCaM) containing 2 M KCl. ^1H, ^{15}N-heteronuclear single quantum correlation (HSQC) spectra were acquired both initially and after every addition of KCl, up to a final concentration of ~340 mM KCl.

NMR Spectroscopy. All spectra were acquired with a Bruker AMX-500 NMR spectrometer operating at a ^1H frequency of 500.14 MHz. All NMR experiments were conducted at 298 K. Parameters for the various NMR experiments employed are shown in Table 1. All heteronuclear experiments were performed on the ^{15}N,^{13}C-labeled samples of apoCaM and the apoCaM–$Neuro_p$ complex. All homonuclear ^1H experiments were performed using unlabeled samples. Except where noted, the sweep width, carrier frequencies, and number of data points acquired were the same for corresponding spectra of both the apoCaM and the complex. High-resolution two-dimensional ^1H–^1H NOESY (Frøystein, 1993), TOCSY (Bax & Davis, 1985), and DQF

Table 1: Summary Description of the Heteronuclear NMR Experiments Employed during the Characterization of Apocalmodulin and the Apocalmodulin·Neuro$_p$ Complex

experiment	pulse sequence	acquired data (complex points) t_3	t_2	t_1	sweep widths (Hz) $\omega 3$	$\omega 2$	$\omega 1$
^{15}N-HSQC[a]	*b*		512 (H)	128 (N)		6410	2016
^{15}N-NOESY-HSQC[c]	*d*	512 (H)	32 (N)	100 (H)[e]	6410	2016	6410
^{15}N-NOESY-HSQC[c]	*d*	512 (H)	35 (N)	100 (H)[f]	6410	2016	6410
HNCA[g]	*h*	512 (H)	56 (C)	32 (N)	6410	3333	2016
HN(CO)CA[i]	*h*	512 (H)	52 (C)	32 (N)	6410	3333	2016
HNCO[g]	*h*	512 (H)	64 (C)	32 (N)	6410	1667	2016
CBCANH[j]	*j*	512 (H)	32 (N)	48 (C)	6410	2016	7692
CB(CO)CANH[k]	*k*	512 (H)	32 (N)	48 (C)	6410	2016	7692
HBHA(CBCACO)NH[l]	*l*	512 (H)	32 (N)	64 (C)[e]	6410	2016	4000
HBHA(CBCACO)NH[l]	*l*	512 (H)	32 (N)	62 (C)[f]	6410	2016	4000
HN(CA)HA[m]	*n*	512 (H)	32 (N)	60 (H)[e]	6410	2016	2000
HN(CA)HA[m]	*n*	512 (H)	32 (N)	62 (H)[f]	6410	2016	2000
HCCH-TOCSY[o,p]	*p*	512 (H)	46 (C)	93 (N)	4000	3333	4000

[a] Bodenhausen and Reuben (1980) [b] Bax et al. (1990) with attenuation of the water resonance by spin locks (Messerle et al., 1989) and ^{13}C-decoupling during t_1 and acquisition. These parameters also apply to spectra acquired for the titration of apoCam with KCl and titration of apoCaM with Neuro$_p$. [c] Fesik and Zuiderweg (1988) and Marion et al. (1989c). [d] The HSQC version of the NOESY-HMQC due to Marion et al. (1989c) was used with a homospoil pulse during the 100-ms NOE mixing time. ^{13}C and ^{15}N-decoupling was employed during t_1 and acquisition and ^{13}C-decoupling during t_2. [e] For apocalmodulin. [f] For the apocalmodulin–Neuro$_p$ complex. [g] Kay et al. (1990). [h] Grzesiek and Bax (1992a) with incorporation of spin locks for additional water suppression. [i] Bax and Ikura (1991). [j] Grzesiek & Bax (1992b). [k] Grzesiek and Bax (1992c). [l] Grzesiek and Bax (1993). [m] Clubb et al. (1992), Boucher et al. (1992), and Olejniczak et al. (1992). [n] The implementation of this pulse sequence was provided by Professor E. R. P. Zuiderweg (personal communication). [o] Fesik et al. (1990). [p] Bax et al. (1990).

COSY (Derome & Williamson, 1990) spectra were also acquired. All experiments employed the States-TPPI method for quadrature detection in the indirectly detected dimensions (Marion et al., 1989a). All spectra were referenced to trace TMS in water (^{1}H, 0.00 ppm), neat TMS (^{13}C, 2.86 ppm), and $^{15}NH_4Cl$ in 1 M HCl (24.93 ppm).

Data Processing and Analysis. Data reduction was accomplished using the FELIX software package (Biosym Technologies). The data were processed by multiplication of the time domain signal in each dimension by a suitable apodizing function (squared shifted cosine or Kaiser), zero-filling, and Fourier transformation. In some cases, additional points in indirectly detected dimensions were predicted using linear prediction (Olejniczak & Eaton, 1990) or mirror-image linear prediction (for constant-time dimensions; Zhu & Bax, 1990). Where appropriate, the water signal component of the FID was removed by a convolution difference method (Marion et al., 1989b). Chemical shift index analysis utilized CSI software due to Wishart and co-workers (Wishart et al., 1991, 1992; Wishart & Sykes, 1994). Amino acid type and sequence probability analysis based on Cα and Cβ chemical shifts (Grzesiek & Bax, 1993) was carried out using software kindly provided by Dr. Stephan Grzesiek.

RESULTS AND DISCUSSION

Titration of Calmodulin with the Neuro$_p$ Peptide. While the affinity of neurogranin for apoCaM is less sensitive to salt (Gerendasy et al., 1995), the binding of the Neuro$_p$ peptide to apocalmodulin is highly sensitive (Chapman et al., 1991) and care must be taken to keep the ionic strength relatively low. The origin of the salt effect appears to be 2-fold: disruption of the ionic interactions between the bound peptide and apocalmodulin (Chapman et al., 1991; Ehrhardt and co-workers, unpublished results) and induction of a conformational change in apoCaM which is incompatible with binding of peptide (see below). The stoichiometric titration of apocalmodulin with the Neuro$_p$ peptide under low-salt conditions was followed by ^{15}N-HSQC spectroscopy. The basic features of the spectral perturbations brought about by binding of the peptide indicate that the complex is in fast exchange with its dissociated components at the NMR concentrations used (~0.5 mM apocalmodulin). The observed dependence of the binding constant on salt concentration (Ehrhardt et al., unpublished observations) indicates that the K_d under the conditions used is ~400 nM. Analysis of chemical shift changes of ^{15}N–^{1}H correlations due to sites that are not undergoing fast hydrogen exchange indicate that the unimolecular dissociation rate is greater than 10^2 s^{-1}. In addition to simple chemical shift effects due to interconversion of free and complexed apocalmodulin on a fast NMR chemical shift time scale, a number of ^{15}N–^{1}H correlations are seen to experience increases in intensity, decreases in line width, and chemical shift changes consistent with a decrease in hydrogen exchange rate upon complexation of the peptide. Most of these sites involve amide hydrogens which are at the ends of helices. The motions leading to hydrogen exchange at these sites are likely dominated by helix–coil transitions, which in turn reflect the intrinsic stability of the involved helical segment. The general slowing of hydrogen exchange at these sites therefore suggests that the binding of the peptide results in a stabilization of the structure. Examples of the spectral effects in the HSQC spectrum of apocalmodulin due to binding of the Neuro$_p$ peptide are shown in Figure 1. The cross peak arising from K148 is a case where the chemical shift perturbation brought about by binding of the peptide occurs without significant line broadening or intensity changes, indicating a case of fast exchange. In this case, the off rate is indicated to be significantly larger than 50 s^{-1}. The more complicated case of chemical changes accompanied by both line width and intensity changes is illustrated by the behavior of the ^{15}N–^{1}H cross peak of L116. Here, the binding of peptide slows hydrogen exchange such that the cross peak becomes observable. This effect is accompanied by a chemical shift change which is averaged by interconversion of free and complexed apocalmodulin. The spectral changes are complete at 1 equiv of peptide, indicating that the 1:1 complex is the predominant form of the complex. Comparison of

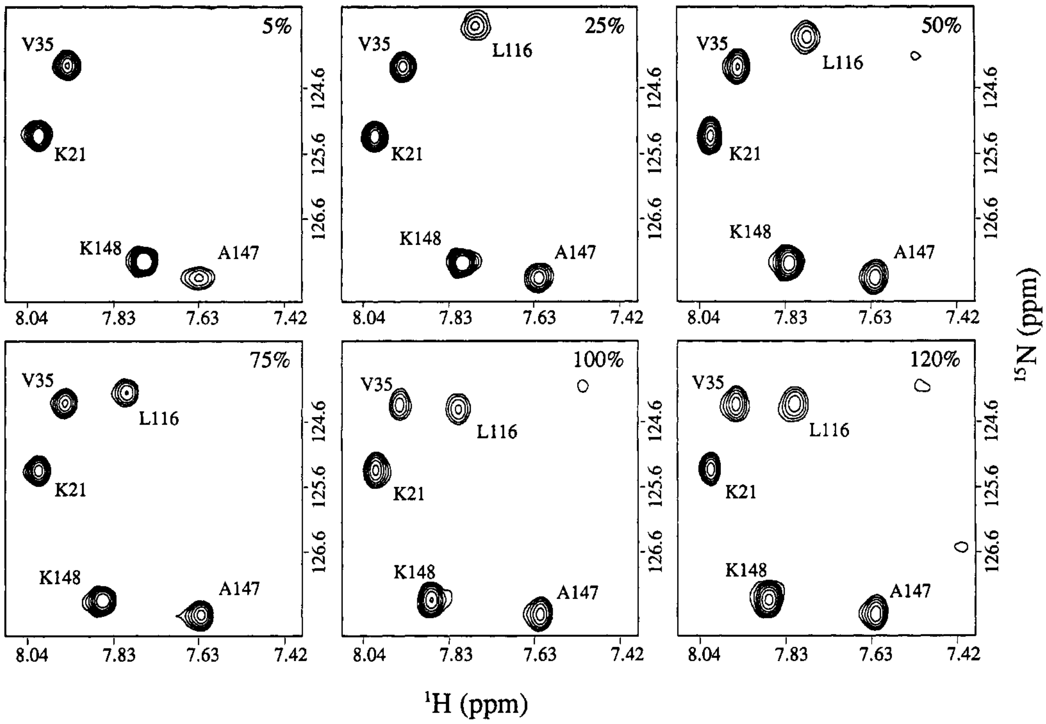

FIGURE 1: Expansions of the ^{15}N-HSQC spectrum of apoCaM during titration with the Neuro$_p$ peptide. The spectra are plotted at identical contour levels. Indicated cross-peak assignments were obtained as described in the text.

the HSQC spectra of both apoCaM and the 1:1 apoCaM•Neuro$_p$ complex reveals significant chemical shift differences throughout apoCaM with the largest differences occurring in the C-terminal domain (see below).

Resonance Assignments. Both apocalmodulin and the apocalmodulin-Neuro$_p$ complex give NMR spectra that lack any significant homology to any previously reported spectra of calcium-loaded CaM or its complex with calmodulin-binding domain peptides [see Ikura et al. (1991a, 1992) and Roth et al. (1992)]. In addition, the crowded spectral features of the ^{15}N-HSQC indicated that a three-step approach to the *de novo* resonance assignment of apoCaM and the apoCaM•Neuro$_p$ complex would be beneficial. As a first step, samples of calmodulin selectively labeled with either α-^{15}N-lysine or α-^{15}N-leucine were prepared and those amino acid types identified in ^{15}N-HSQC spectra of apoCaM and the apoCaM•Neuro$_p$ complex in order to provide independent reference points on the main chain (Figure S1 in the supporting information). This approach has been used previously with great success (McIntosh et al.,1990; Roth et al., 1992) and here yielded 17 contact points for a resonance assignment strategy based on interresidue correlation via triple resonance spectroscopy and one based on interresidue connectivities via NOE-correlation spectroscopy.

The bulk of the resonance assignments reported here were obtained using the standard library of triple resonance NMR experiments (Bax & Grzesiek, 1993). The information obtained from the HNCA, HN(CO)CA, HN(CA)HA, HBHA-(CBCACO)NH, CBCANH, and CBCA(CO)NH experiments allowed the correlation of the amide proton and amide nitrogen chemical shifts of a given amino acid to the Cα, Cβ, and Hα resonances of both the same and previous residues in the primary sequence. Examples of relatively straightforward interresidue correlations in ApoCaM by use of HN(CO)CA and HNCA spectra are shown in Figures S2 and S3 (in the supporting information). Examples of the use of the CBCA(CO)NH and CBCANH pair of experiments to establish interresidue connectivities in the apoCaM•Neuro$_p$ complex are shown in Figures S4 and S5 (in the supporting information). The third set of experiments, HBHA(CBCA-CO)NH and HN(CA)HA, reference the same amide nitrogen and hydrogen resonances as the previous experiments but establish the interresidue linkage via the Hα. In addition, the HBHA(CBCACO)NH yielded assignments of the Hβ resonances. For apoCaM, all three interresidue correlations were observed 51% of the time, only two interresidue correlations were seen 33% of the time, and only one interresidue correlation was observed 16% of time. Similar results were obtained for the complex. From these data sets, the backbone resonances of 55% of amino acid residues of apoCaM and the apoCaM•Neuro$_p$ complex could be directly assigned without reference to other information. As described below, reference to interresidue NOEs, side-chain assignments, selectively labeled samples, and characterization of amino acid type by chemical shift analysis was required to obtain the balance of the resonance assignments. The HCCH-TOCSY experiment was used to provide sufficient side-chain ^{1}H and ^{13}C assignments to verify amino acid type assignments in most cases.

There were a number of instances where significant degeneracy in the α carbon or the absence of interresidue correlations required the use of ^{15}N-resolved NOESY spectra to complete the sequence-specific assignments. Many of the apparent ambiguities in interresidue linkage could be resolved by appealing to the interresidue NH(i)$-$NH(i $-$ 1) NOE correlations available in helical segments (Wüthrich et al., 1984; Wand & Nelson, 1991). An example of how a Cα degeneracy in the HN(CO)CA spectrum of apoCaM was resolved by the presence of an interresidue NH(i)$-$NH(i $-$ 1) NOE is shown in Figure S6 (in the supporting information). Confidence in this approach rests on the high degree of correlation between regular secondary structure and more

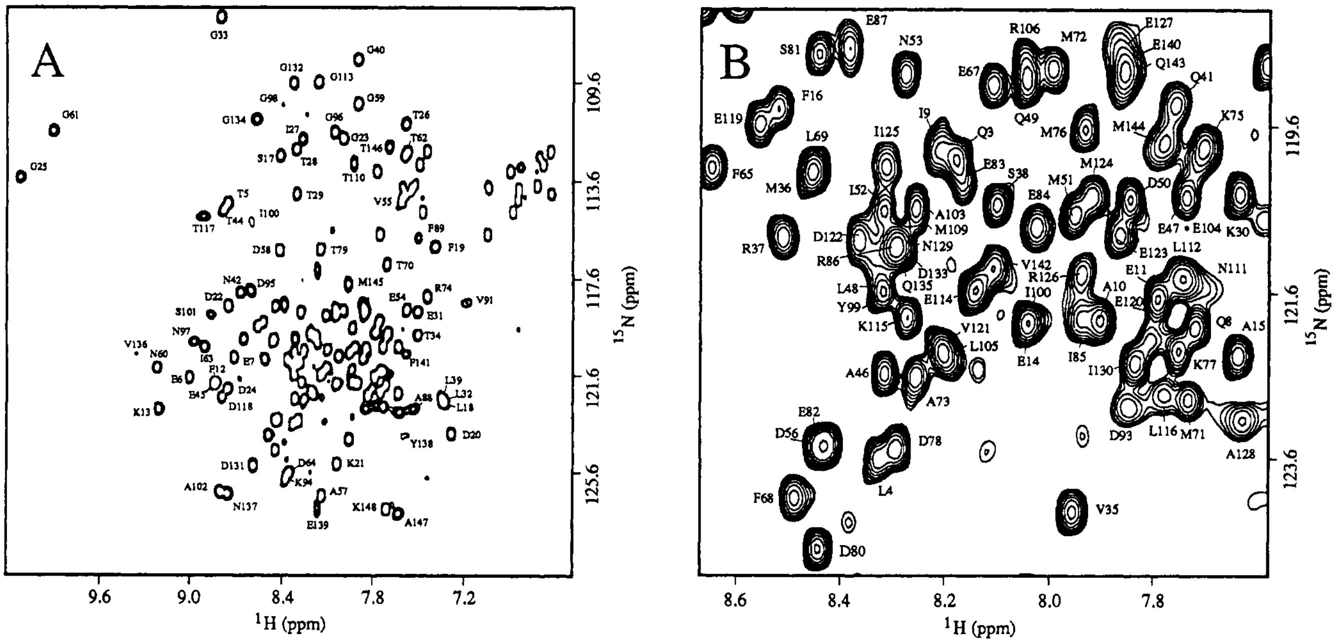

FIGURE 2: ^{15}N-HSQC spectrum of apocalmodulin obtained at 25 °C and pH 6.5. The indicated cross-peak assignments were obtained as described in the text. Panel A is the full spectrum while Panel B is an expansion of the most crowded region.

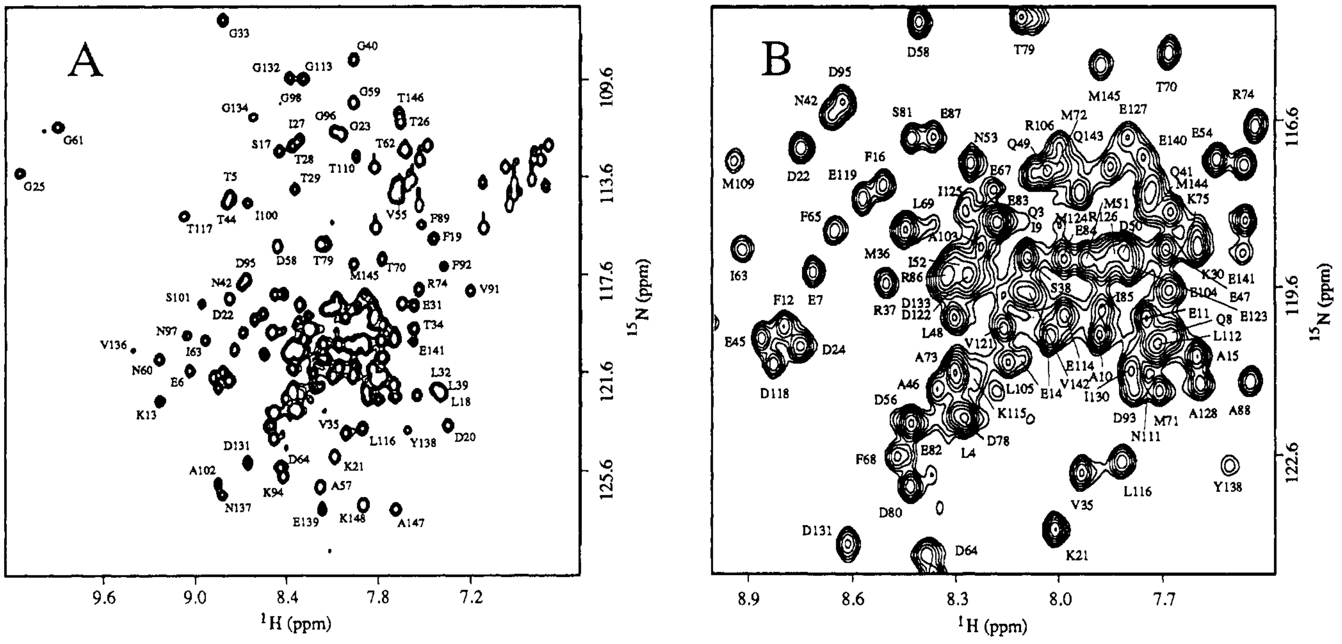

FIGURE 3: ^{15}N-HSQC spectrum obtained at 25 °C and pH 6.5 of apocalmodulin in 1:1 complex with the Neuro$_p$ peptide. The indicated cross-peak assignments were obtained as described in the text. Panel A is the full spectrum while Panel B is an expansion of the most crowded region.

extensive interresidue NOE sets such as those defined by the main-chain-directed assignment library of NOE patterns (Wand & Nelson, 1991). Obviously, this strategy works best when dealing with areas of well-defined α-helical or β-sheet secondary structure, where MCD patterns can be used to the best effect. In this instance, the NOE data were far more useful for assigning resonances in the N-terminal domains of both apoCaM and the apoCaM•Neuro$_p$ complex than in the C-terminal domains (see below and Figures 4 and 5). Additional support for the resonance assignments obtained comes from an analysis based on sequence probabilities determined from sequential Cα and Cβ chemical shifts (Grzesiek & Bax, 1993). As a final approach, the parallel assignment of the apoCaM and the apoCaM•Neuro$_p$ complex also enabled resolution of many degeneracies. Because of the fast exchange behavior during titration of apoCaM with the peptide, cross assignment between the two states was possible in many instances where ambiguities in one state were resolved in the other. This also allowed complete assignment of all carbonyl carbon resonances using only the HNCO experiment for both apoCaM and the apoCaM•Neuro$_p$ complex. Sequence-specific ^{15}N–^{1}H cross-peak assignments obtained in this work are summarized in Figures 2 and 3. Unassigned resonances in the upper right-hand corner represent side-chain amide groups, while arginine guanidino groups are aliased and appear as negative contours. The complete backbone assignments for both states of calmodulin are given in Tables S1 and S2 of the supporting information.

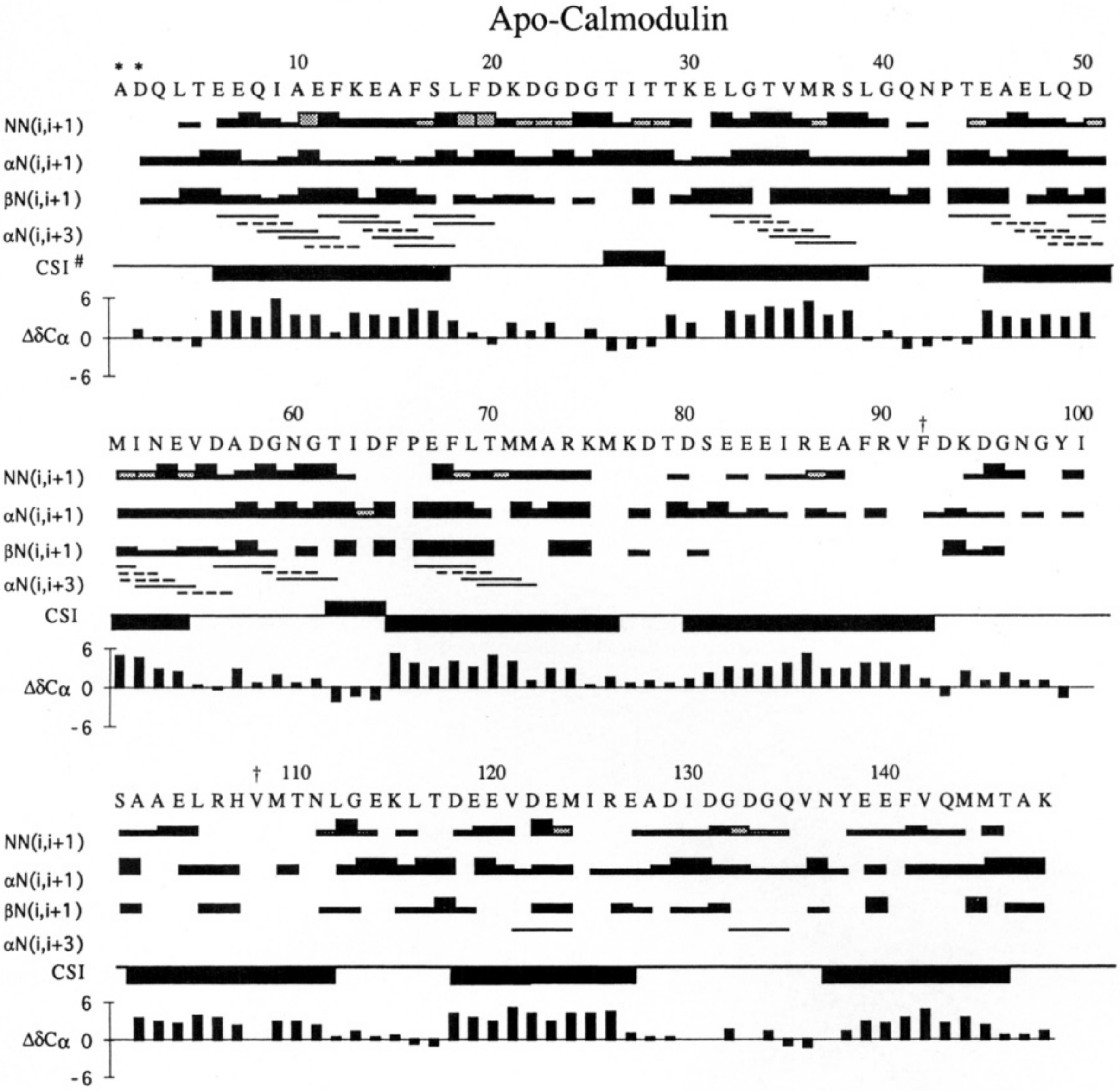

FIGURE 4: Summary of the consensus chemical shift index (Wishart et al., 1991, 1992; Wishart & Sykes, 1994) and the short-, medium-, and long-range NOE's involving HN, Hα, and Hβ for apocalmodulin obtained using an NOE mixing time of 100 ms. Solid boxes and lines represent resolved NOE's. Stippled boxes and dashed lines indicate the presence of a potential contribution from a degeneracy. Asterisks indicate main-chain and side-chain resonance assignments were undetermined. Daggers indicate side-chain resonances were assigned, but main-chain amide ^{15}N and ^{1}H resonance assignments were not determined or tentative. Number signs indicate that the chemical shift index utilized ^{1}Hα, ^{13}Cα, ^{13}Cβ, and ^{13}CO resonance assignments.

Structure of the Globular Domains. ^{15}N-NOESY-HSQC spectra collected with 100-ms mixing times were examined for main-chain NOEs arising from short distance interactions typical of regular secondary structure. Figures 4 and 5 present a summary of NOE's observed between amide hydrogens and amide α and β hydrogens of apoCaM and the apoCaM•Neuro$_p$ complex. Also shown are the consensus chemical shift index (Wishart & Sykes, 1994) and α carbon chemical shift differences from the random coil values (Spera & Bax, 1991). An interesting result is obtained. The N-terminal globular domain of calmodulin (residues 1−64) in both states has much better defined regular secondary structure by either MCD or chemical shift analysis criteria than does the C-terminal globular domain (residues 94−148). The helices of the two EF-hands of the N-terminal domain show the extensive network of strong intra- and interresidue NOEs indicative of regular helical structure, in particular the (i, i + 3) interactions (Wand & Nelson, 1991). The completeness of the NOE patterns is especially important in light of the incompleteness seen in corresponding EF-hand regions of the C-terminal domain. In the C-terminal domain, the density of main-chain NOEs is generally much sparser both in the apoprotein and in the complex. The MCD pattern analysis fails to assign large units of regular helical structure in the C-terminal domain of both apoCaM and the apoCaM•Neuro$_p$ complex. Nevertheless, helical structure is indicated by the presence of sequential amide−amide NOEs. Regular helical secondary structure is clearly indicated by the CSI analysis of the C-terminal domain. The apparent inconsistency between the observed pattern of NOEs and the chemical shift analysis strongly indicates that considerable motion is present. The motional sensitivities of the chemical shift and the NOE are quite different, with the former essentially being a simple average of the chemical shifts of the populations being sampled while the NOE has a highly nonlinear dependence upon structure (distance).

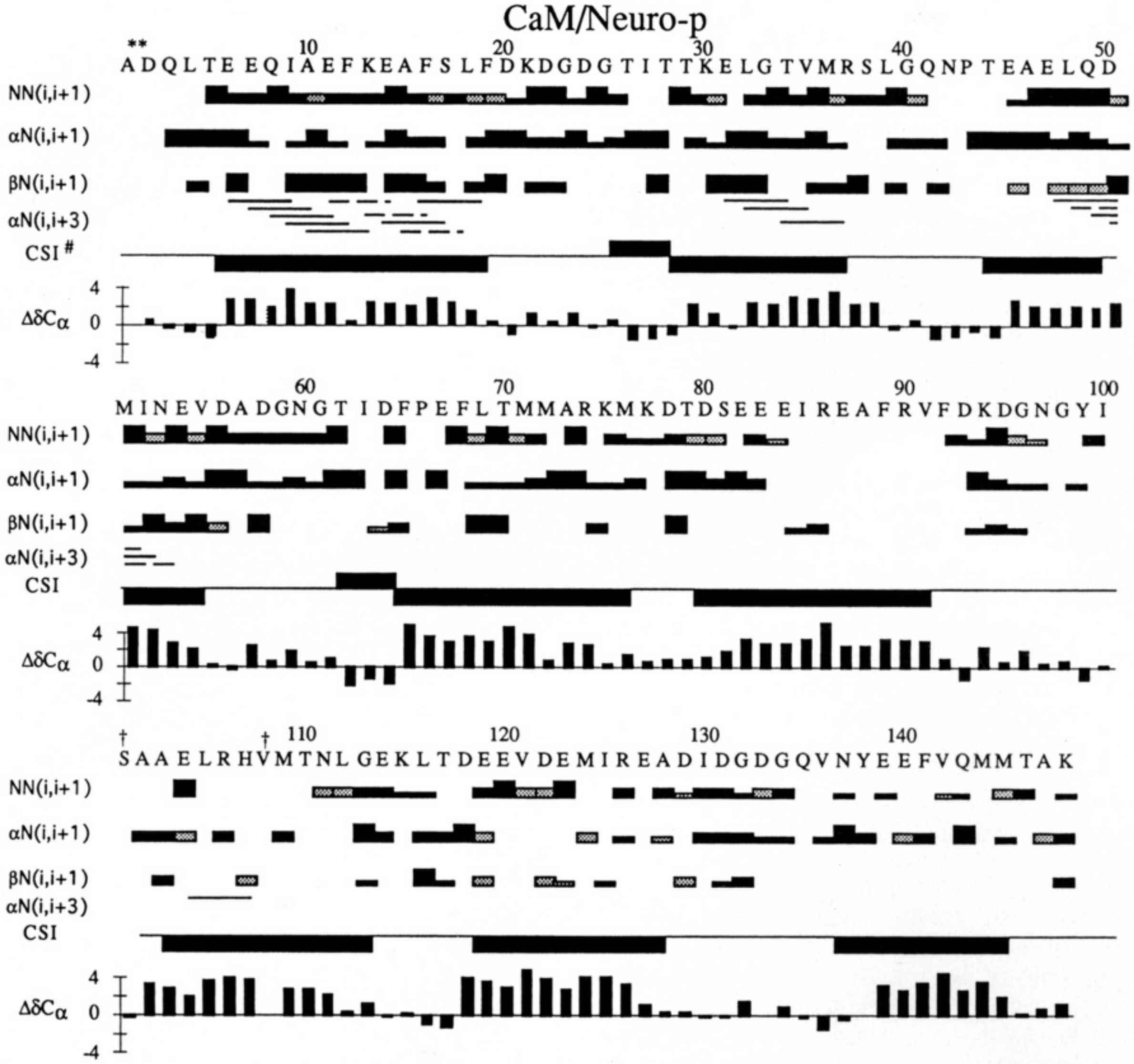

FIGURE 5: Summary of the consensus chemical shift index (Wishart et al., 1991, 1992; Wishart & Sykes, 1994) and the short-, medium-, and long-range NOE's involving HN, Hα, and Hβ for the apocalmodulin/neuromodulin complex. Symbols are as described for Figure 4.

Nevertheless, all of the identified helical elements of apoCaM or the complex are present in the calcium-loaded calmodulin (Ikura et al., 1991b). The β-strands of the EF-hand motifs are present in both domains in both apoCaM and its complex with $\mathrm{Neuro_p}$. Interstrand NOEs characteristic of antiparallel β-sheet structure are seen in the N-terminal domain in complete analogy to the calcium-saturated state. The tertiary organization of the N-terminal domain is also highly homologous as indicated by the observation of a number of NOEs predicted by the structure of the calcium-loaded state (Babu et al., 1988) to occur between the side chains of aromatic and aliphatic residues such as F19 and V35, I27 and F16 and F68, and L32 and F19, for example (not shown). In contrast, interstrand NOEs characteristic of antiparallel β-sheet structure are not seen in the C-terminal domain even at relatively long mixing times (130 ms) under low-salt conditions (see below). For example, the long-distance interstrand NH–CαH and NH–NH NOEs characteristic of β-sheet structure are seen in the N-terminal domain of both apoCaM and the complex but are absent in the C-terminal domain under low-salt conditions. Also absent in the C-terminal domains of both apoCaM and the complex are the NOEs expected for the much shorter interstrand Hα–Hα distance typical of β-sheet structure. NOE contacts between aromatic and aliphatic side chains predicted from the calcium-saturated structure are also not present in the C-terminal domain of apCaM (F89, F92, I100, F141), again in contrast to the N-terminal domain. Furthermore, these and other residues of the hydrophobic core of the C-terminal domain of apoCaM (L105, V108, M144) give only weak interresidue main-chain connectivities, which is consistent with extensive motion even on the main chain. These results are somewhat different from those obtained from studies of the apo form of isolated C-terminal domain of calmodulin (Finn et al., 1993). Many of the NOE contacts seen in the study of the C-terminal domain fragment were not observed in the C-terminal domain of apoCaM. These include most of the NOEs between hydrophobic core residues in this domain, as noted above, whose side chains are presumably shielded from solvent in apoCaM and exposed upon binding of calcium. These differences may reflect a dependence on specific interactions with the rest of the molecule (i.e., the central helix region or the N-terminal domain). These observations are consistent with the notion of direct or indirect interdomain interactions in apoCaM which have structural consequences (Pedigo & Shea, 1995). Coupled with the fact that the aromatic rings of the C-terminal domain noted above are averaged, these observations also suggest that this domain is more dynamic and loosely packed.

Integrity of the Central Helix. The long central helix bridging the two globular domains seen in the crystal has been shown to be largely present in solution but locally disordered in its central region (Ikura et al., 1991b; Barbato et al., 1992). Only one of the two resulting α helices is present in the apo state of the protein. The majority of the helix encompassing residues F65−K77 in calcium-loaded CaM (Ikura et al., 1991b) is present in apoCaM, while the second helical segment encompassing residues E82−D93 shows NOE patterns consistent with a highly averaged backbone conformation. Upon binding of peptide, the (*i*, *i* + 3) αN NOEs, characteristic of a tight regular helical secondary structure, are no longer seen in the helix spanning residues F65−K77 in apoCaM. Indeed, the pattern of main-chain NOEs observed in this region is irregular, indicating a highly averaged structure. Again, the chemical shift analysis indicates that the average structure throughout this region is helical (Figure 5). The C-terminal portion of the central helix (residues 82−92) is almost devoid of main-chain NOEs in the apoCaM•Neuro$_p$ complex. Thus the binding of the peptide extensively disrupts the central helix.

Effects of the Binding of Calcium to Apocalmodulin. The secondary structure of the calcium-saturated state of calmodulin has been characterized by both NMR (Ikura et al., 1991b) and X-ray crystallography (Babu et al., 1988). The resonance assignments and NOE data presented here offer the opportunity to extend earlier investigations of the structural effects of the binding of calcium to the apoprotein [e.g., Seamon et al. (1980) and Klevit et al. (1984)]. Comparison of the chemical shift indices and patterns of main-chain NOEs of the two states of CaM indicates that the binding of calcium has the most dramatic effect in the C-terminal domain, the domain having the highest calcium-binding affinity (Minowa et al., 1984). All four of the loosely helical segments of the two EF-hand motifs of the C-terminal domain become more regular in their helical structure as indicated by the more extensive interresidue NOE network and unambiguous helical chemical shift index [see Figure 8 of Ikura et al. (1991b)]. The changes in the N-terminal domain are more subtle with only a slight lengthening of the consensus boundaries of helical secondary structure. The central helix becomes better defined especially its C-terminal segment, involving residues 82−93, which is irregular in apoCaM. There are no apparent contacts between the two globular domains in the calcium-saturated state, presumably because of the restriction of dynamic disorder to a few residues in the middle of the central helix (Ikura et al., 1991b). These general effects of ordering of the protein are consistent with earlier observations and speculations on the effect of metal ligand binding.

Effects of the Binding of Neuro$_p$ to Apocalmodulin. The chemical shift perturbations of apoCaM brought about by the binding of the Neuro$_p$ peptide are generally localized to the C-terminal domain (Figure 6). Several interesting features emerge. For example, the carbonyl carbon resonances in the putative helical regions mostly experience a downfield shift upon binding of the peptide. This is consistent with increased hydrogen-bond stability, which in turn is reflected in the slowed hydrogen exchange noted above. Curiously, the α-carbon shift changes are uniformly upfield in the putative helical regions of the protein upon binding of the peptide. This is consistent with the time-averaged decrease in helicity upon binding of the peptide. Nevertheless, a general ordering and stabilization of the C-terminal domain by the binding of peptide is indicated, though it is clearly less extensive than that induced by the binding of calcium. The localization of significant structural perturbations to the C-terminal domain is reminiscent of the interaction of trifluoperazine with calcium-saturated calmodulin, where the drug makes extensive contacts with residues in the C-terminal domain but relatively few contacts with the N-terminal domain (Cook et al., 1994).

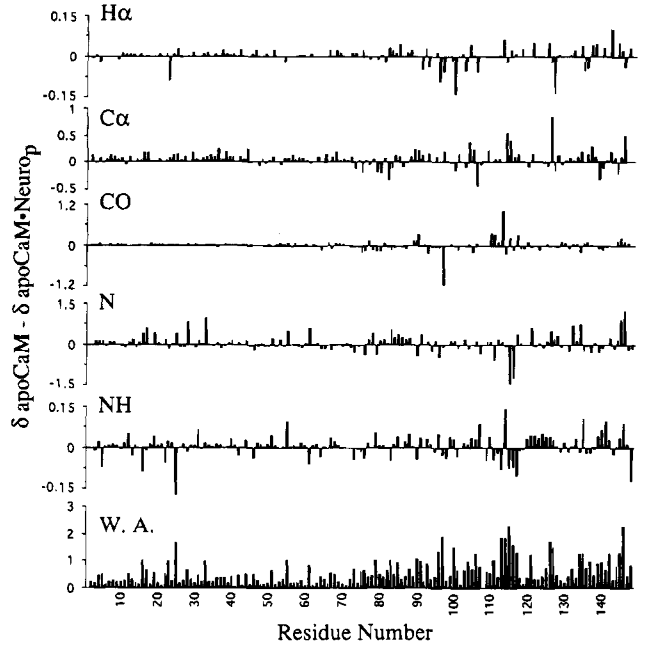

FIGURE 6: Summary of the chemical shift changes in apocalmodulin brought about by the binding of the Neuro$_p$ peptide. Shown are the changes in chemical shift experienced by α hydrogen and carbon, carbonyl carbon, amide nitrogen, and hydrogen resonances upon binding of the peptide to apoCaM. The bottom panel shows a simple weighted average of the chemical shift changes at each site.

Effects of the Binding of Calcium to the Apocalmodulin•Neuro$_p$ Complex. The putative physiological role of calmodulin with respect to neurogranin and neuromodulin is to sequester these proteins under low calcium conditions (Masure et al., 1986; Liu & Storm, 1989). As mentioned above, the intact proteins bind to apoCaM with high affinity and do not bind with appreciable affinity to calcium-saturated CaM. In contrast, the isolated peptides corresponding to the calmodulin-binding domains of the two proteins and the analogue used here (Neuro$_p$) do bind to calcium-saturated CaM. Thus, the model peptides offer the opportunity to examine the origins of the calcium-dependent binding of peptide. As illustrated here, the binding of calcium and peptide can be separately examined, providing a unique opportunity to dissect the linkage between the two functions of the protein: the binding of calcium and the binding of a target domain. Importantly, the binding of calcium to an apoCaM−peptide complex can be examined. Figure 7 illustrates some of the effects of the binding of calcium on the apoCaM•Neuro$_p$ complex. Calcium binding under NMR conditions is in slow exchange. The stoichiometric binding of calcium to the EF-hands of the two globular domains of the complex is clearly discrete as the resonances of the

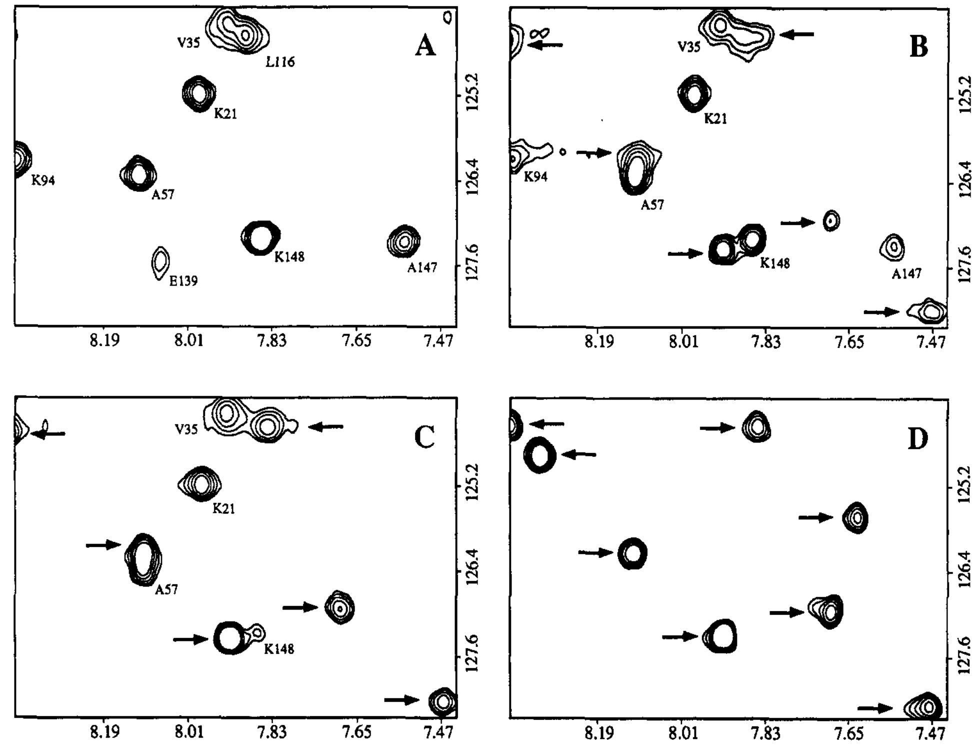

FIGURE 7: Titration of the apoCaM•Neuro$_p$ complex with calcium. Shown are ^{15}N-HSQC spectra of the apoCaM•Neuro$_p$ complex in the presence of ~0.2 equiv (panel A), ~1 equiv (panel B), ~1.8 equiv (panel C), and ~4.4 equiv of calcium (panel D). Cross peaks from selected residues in the N- and C-terminal domains of calmodulin are shown. Arrows indicate cross peaks arising from a calcium-loaded state of calmodulin. Compare to the ^{15}N-HSQC spectrum of apoCaM shown in Figure 2.

C-terminal domain of the complex are affected first. For example, as shown in Figure 7, the cross peaks arising from K94, L116, E139, A147, and K148 in apoCaM are no longer observable after the addition of ~2 equiv of calcium, whereas those of K21, V35, and A57 are essentially unperturbed. The latter set of resonances of the N-terminal domain are only signficantly affected when more than 2 equiv of calcium has bound. Thus, the free energy associated with the binding of the peptide to apoCaM and its concomitant structural ordering of the C-terminal domain has maintained and perhaps enhanced that domain's binding affinity for calcium relative to the N-terminal domain. A similar transmission of free energy from peptide binding to calcium binding has been observed in the interaction of calmodulin with a peptide based upon the calmodulin-binding domain of the skeletal muscle myosin light-chain kinase (Seeholzer & Wand, 1989).

Effect of Salt on Apocalmodulin. The interaction of Neuro$_p$ with apoCaM is sensitive to salt (Chapman et al., 1991). The structure of apoCaM itself also appears to be sensitive to ionic strength. As the KCl concentration is increased, there is a small change in the chemical shifts of most resonances, as would be expected. This effect continues as the ionic strength is increased to over 300 mM. More interesting is the appearance of new peaks as the KCl concentration is increased. Both these effects are illustrated in the expansions of HSQC spectra shown in Figure 8. For those resonances which appear as the ionic strength is increased, the concentration of KCl at which a given peak appears at 50% its maximal volume ranges from 30 to 75 mM, while the corresponding range for 75% maximal volume is 60–150 mM. These data indicate the presence of a significantly heterogenous population at physiological salt concentrations. At high salt concentrations, interstrand NOEs are seen between the loops of the two EF-hands of the C-terminal domain, indicating the presence of β-sheet structure in constrast to the results obtained under low-salt conditions (see above).

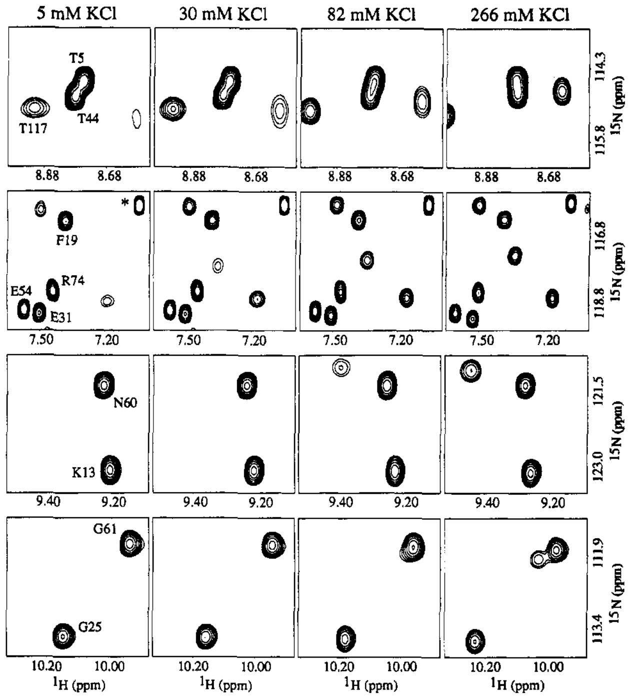

FIGURE 8: Effect of ionic strength on apocalmodulin. Shown are selected regions of ^{15}N-HSQC spectra acquired at increasing total KCl concentrations. Cross peaks assigned at low ionic strength are indicated. Cross peaks appearing at increased KCl concentrations are unassigned. The peak marked with an asterisk is an unassigned side-chain resonance.

Summary and Concluding Remarks. The examination of the effects of the binding of calcium and a regulatory domain peptide analogue to apocalmodulin has allowed characterization of the structural changes brought about by each and the energetic consequences of one on the other. The Neuro$_p$ peptide used here has sufficient binding affinity for both apoCaM and calcium-saturated CaM such that the separation and recombination of the two classes of binding is possible. It has been shown that the N-terminal domain of apoCaM is highly ordered and has secondary and tertiary structural organization homologous to that of calcium-saturated calmodulin. The C-terminal domain of apoCaM is less well defined in terms of both secondary and tertiary structure, in contrast to results previously reported for a tryptic fragment of CaM (Finn et al., 1993). In particular, the β-sheet structure formed between the loops of each EF-hand of the C-terminal domain in calcium-saturated calmodulin is not present in either apoCaM or the apoCaM·Neuro$_p$ complex. NOEs anticipated on the basis of the model proposed by Finn et al. (1993) are not seen, and several NOEs between side chains suggest that the core of the C-terminal domain is more solvent-exposed, dynamic, and closer to the calcium-saturated state than previously thought. Nevertheless, the details of the tertiary structure remain to be determined. Hydrogen exchange behavior, relaxation data (NOE), and chemical shift data suggest that the C-terminal domain is also relatively dynamically disordered, which is consistent with earlier results (Török et al., 1992). The binding of the peptide to apoCaM causes a nominal ordering of the the C-terminal domain, a reduction in average helicity of the C-terminal portion of the "central helix", and a stabilization of the remaining helical structure. The binding of the Neuro$_p$ peptide to apoCaM appears to result in only a modest reorganization of the globular domains of the protein. Though no interdomain contacts have been found, the degree to which the complex has collapsed to a compact state cannot be unequivocally characterized at this point. Nevertheless, the binding of peptide does cause the calcium-binding affinities of the two domains to become sufficiently different such that the two domains can be discretely filled with metal ligand.

ACKNOWLEDGMENT

We are grateful to Ms. Ramona Bieber for advice and technical assistance throughout this work. We also thank Dr. Peter Flynn for several helpful discussions, Dr. Stephan Grzesiek for guidance, and Professor E. R. P. Zuiderweg for sharing his implementation of the HN(CA)HA pulse sequence.

SUPPORTING INFORMATION AVAILABLE

Two tables of assigned chemical shifts for apocalmodulin and the apocalmodulin–Neuro$_p$ complex and six figures showing the assignment of residue type by use of selectively labeled calmodulin and illustrations of the use of triple resonance and NOE-based spectroscopy to assign the two states of calmodulin (18 pages). Ordering information is given on any current masthead page.

REFERENCES

Apel, E. D., Byford, M. F., Au, D., Walsh, K. A., & Storm, D. R. (1990) *Biochemistry 29*, 2330–2335.

Aulabaugh, A., Niemczura, W. P., Blundell, T. L., & Gibbons, W. A. (1984) *Eur. J. Biochem. 143*, 409–418.

Babu, Y. S., Bugg, C. E., & Cook, W. J. (1988) *J. Mol. Biol. 204*, 191–204.

Barbato, G., Ikura, M., Kay, L. E., Pastor, R. W., & Bax, A. (1992) *Biochemistry 31*, 5269–5278.

Baudier, J., Deloulme, J. C., Dorrselaer, A. V., Black, D., & Matthes, H. W. D. (1991) *J. Biol. Chem. 266*, 229–237.

Bax, A., & Davis, D. G. (1985) *J. Magn. Reson. 65*, 355–360.

Bax, A., & Ikura, M. (1991) *J. Biomol. NMR 1*, 99–104.

Bax, A., & Grzesiak, S. (1993) *Acc. Chem. Res. 26*, 131–138.

Bax, A., Clore, G. M., & Gronenborn, A. M. (1990) *J. Magn. Reson. 88*, 425–431.

Bodenhausen, G., & Reuben, D. J. (1980) *Chem. Phys. Lett. 69*, 185–189.

Boucher, W., Laue, E. D., Campbell-Burk, S. L., & Domaille, P. J. (1992) *J. Biomol. NMR 2*, 631–637.

Budesinsky, B. W. (1974) *Anal. Chim. Acta 71*, 343–347.

Chapman, E. R., Au, D., Alexander, K. A., Nicolson, T. A., & Storm, D. R. (1991) *J. Biol. Chem. 266*, 207–213.

Clubb, R. T., Thanabal, V., & Wagner, G. (1992) *J. Biomol. NMR 2*, 203–210.

Cook, W. J., Walter, L. J., & Walter, M. R. (1994) *Biochemistry 33*, 15259–15265.

Derome, A. E., & Williamson, M. P. (1990) *J. Magn. Reson. 88*, 177–185.

Ehrhardt, M. R., Urbauer, J. L., & Wand, A. J. (1995) *Biochemistry* (in press).

Fesik, S. W., & Zuiderweg, E. R. P. (1988) *J. Magn. Reson. 78*, 588–593.

Fesik, S. W., Eaton, H. L., Olejniczak, E. T., & Zuiderweg, E. R. P. (1990) *J. Am. Chem. Soc. 112*, 886–888.

Finn, B. E., Drakenberg, T., & Forsén, S. (1993) *FEBS Lett. 336*, 368–374.

Fisher, P. J., Prendergast, F. G., Ehrhardt, M. E., Urbauer, J. L., Wand, A. J., Sedarous, S. S., McCormick, D. J., & Buckley, P. J. (1994) *Nature 368*, 361–363.

Frøysten, N. Å. (1993) *J. Magn. Reson., Ser. A 103*, 332–337.

Gerendasy, D. D., Herron, S. R., Jennings, P. A., & Sutcliffe, J. G. (1995) *J. Biol. Chem. 270*, 6741–6750.

Gopalakrishna, R., & Anderson, W. B. (1982) *Biochem. Biophys. Res. Commun. 104*, 830–836.

Grzesiek, S., & Bax, A. (1992a) *J. Magn. Reson. 96*, 432–440.

Grzesiek, S., & Bax, A. (1992b) *J. Magn. Reson. 99*, 201–207.

Grzesiek, S., & Bax, A. (1992c) *J. Am. Chem. Soc. 114*, 6291–6293.

Grzesiek, S., & Bax, A. (1993) *J. Biomol. NMR 3*, 185–204.

Hennessey, J. P., Jr., Manavalan, P., Johnson, W. C., Jr., Malencik, D. A., Anderson, S. R., Schimerlik, M. I., & Shalitin, Y. (1987) *Biopolymers 26*, 561–571.

Ikura, M., Kay, L. E., & Bax, A. (1990) *Biochemistry 29*, 4659–4667.

Ikura, M., Kay, L. E., Krinks, M., & Bax, A. (1991a) *Biochemistry 30*, 5498–5504.

Ikura, M., Spera, S., Barbato, G., Kay, L. E., Krinks, M., & Bax, A. (1991b) *Biochemistry 30*, 9216–9228.

Ikura, M., Clore, G. M., Gronenborn, A. M., Zhu, G., Klee, C. B., & Bax, A. (1992) *Science 256*, 632–638.

Kay, L. E., Ikura, M., Tschudin, R., & Bax, A. (1990) *J. Magn. Reson. 89*, 496–514.

Klevit, R. E., Dalgarno, D. C., Levine, B. A., & Williams, R. J. P. (1984) *Eur. J. Biochem. 139*, 109–114.

Liu, Y., & Storm, D. R. (1989) *J. Biol. Chem. 264*, 12800–12804.

Marion, D., Ikura, M., Tschudin, R., & Bax, A. (1989a) *J. Magn. Reson. 85*, 393-399.

Marion, D., Ikura, M., & Bax, A. (1989b) *J. Magn. Reson. 84*, 425–430.

Marion, D., Kay, L. E., Sparks, S. W., Torchia, D. A., & Bax, A. (1989c) *J. Am. Chem. Soc. 111*, 1515–1517.

Martin, S. R., & Bayley, P. M. (1986) *Biochem. J. 238*, 485–490.

Masure, H. R., Alexander, K. A., Wakim, B. T., & Storm, D. R. (1986) *Biochemistry 25*, 7553–7560.

Maune, J. F., Beckingham, K., Martin, S. R., & Bayley, P. M. (1992) *Biochemistry 31*, 7779–7786.

McIntosh, L. P., Wand, A. J., Lowry, D. F., Redfield, A. G., & Dahlquist, F. W. (1990) *Biochemistry 29*, 6341–6362.

Meador, W. E., Means, A. R., & Quiocho, F. A. (1992) *Science 257*, 1251–1255.

Meador, W. E., Means, A. R., & Quiocho, F. A. (1993) *Science 262*, 1718−1721.

Messerle, B. A., Wider, G., Otting, G., Weber, C., & Wüthrich, K. (1989) *J. Magn. Reson. 85*, 608−613.

Minowa, O., & Yagi, K. (1984) *J. Biochem. (Tokyo) 96*, 1175−1182.

Olejniczak, E. T., & Eaton, H. L. (1990) *J. Magn. Reson. 87*, 628−632.

Olejniczak, E. T., Xu, R. X., Petros, A. M., & Fesik, S. W. (1992) *J. Magn. Reson. 100*, 444−450.

O'Neil, K. T., & De Grado, W. F. (1990) *Trends Biochem. Sci. 15*, 59−64.

Pedigo, S., & Shea, M. A. (1995) *Biochemistry 34*, 1179−1196.

Pereschini, A., & Kretsinger, R. H. (1988) *J. Biol. Chem. 263*, 12175−12178.

Putkey, J. A., Slaughter, G. R., & Means, A. R. (1985) *J. Biol. Chem. 260*, 4704−4712.

Roth, S. M., Schneider, D. M., Strobel, L. A., Van Berkum, M. F. A., Means, A. R., & Wand, A. J. (1991) *Biochemistry 30*, 10078−10084.

Roth, S. M., Schneider, D. M., Strobel, L. A., Van Berkum, M. F. A., Means, A. R., & Wand, A. J. (1992) *Biochemistry 31*, 1443−1451.

Seamon, K. B. (1980) *Biochemistry 19*, 207−215.

Seeholzer, S. H., & Wand, A. J. (1989) *Biochemistry 28*, 4011−4020.

Spera, S., & Bax, A. (1991) *J. Am. Chem. Soc. 113*, 5490−5492.

Spera, S., Ikura, M., & Bax, A. (1991) *J. Biomol. NMR 1*, 155−165.

Starovasnik, M. A., Su, D.-R., Beckingham, K., & Klevit, R. E. (1992) *Protein Sci. 1*, 245−253.

Török, K., Lane, A. N., Martin, S. R., Janot, J.-M., & Bayley, P. M. (1992) *Biochemistry 31*, 3452−3462.

Wand, A. J., & Nelson, S. J. (1991) *Biophys. J. 59*, 1101−1112.

Wishart, D. S., & Sykes, B. D. (1994) *J. Biomol. NMR 4*, 171−180.

Wishart, D. S., Sykes, B. D., & Richards, F. M. (1991) *J. Mol. Biol. 222*, 311−333.

Wishart, D. S., Sykes, B. D., & Richards, F. M. (1992) *Biochemistry 31*, 1647−1651.

Wüthrich, K., Billeter, M., & Braun, W. (1984) *J. Mol. Biol. 180*, 715−740.

Yao, Y., Schöneich, C. & Squier, T. C. (1994) *Biochemistry 33*, 7797−7810.

Zhang, M., Vogel, H. J., & Zwiers, H. (1994) *Biochem. Cell. Biol. 72*, 109−116

Zhu, G., & Bax, A. (1990) *J. Magn. Reson. 90*, 405−410.

BI950465F